

A silazane additive for $CsPbI_2Br$ perovskite solar cells

Ruiqi Cao(曹瑞琪), Yaochang Yue(乐耀昌), Hong Zhang(张弘), Qian Cheng(程倩), Boxin Wang(王博欣), Shilin Li(李世麟), Yuan Zhang(张渊), Shuhong Li(李书宏), and Huiqiong Zhou(周惠琼)

Citation: Chin. Phys. B, 2022, 31 (**11**): 110101. DOI: 10.1088/1674-1056/ac7c01

Journal homepage: http://cpb.iphy.ac.cn; http://iopscience.iop.org/cpb

What follows is a list of articles you may be interested in

SiO_2 nanoparticle-regulated crystallization of lead halide perovskite and improved efficiency of carbon-electrode-based low-temperature planar perovskite solar cells

Zerong Liang(梁泽荣), Bingchu Yang(杨兵初), Anyi Mei(梅安意), Siyuan Lin(林思远), Hongwei Han(韩宏伟), Yongbo Yuan(袁永波), Haipeng Xie(谢海鹏), Yongli Gao(高永立), Conghua Zhou(周聪华)

Chin. Phys. B, 2020, 29 (**7**): 078401. DOI: 10.1088/1674-1056/ab8da5

Promise of commercialization: Carbon materials for low-cost perovskite solar cells

Yu Cai(蔡宇), Lusheng Liang(梁禄生), Peng Gao(高鹏)

Chin. Phys. B, 2018, 27 (**1**): 018805. DOI: 10.1088/1674-1056/27/1/018805

Novel hole transport layer of nickel oxide composite with carbon for high-performance perovskite solar cells

Sajid, A M Elseman, Jun Ji(纪军), Shangyi Dou(窦尚轶), Hao Huang(黄浩), Peng Cui(崔鹏), Dong Wei(卫东), Meicheng Li(李美成)

Chin. Phys. B, 2018, 27 (**1**): 017305. DOI: 10.1088/1674-1056/27/1/017305

O_3 fast and simple treatment-enhanced p-doped in Spiro-MeOTAD for CH_3NH_3I vapor-assisted processed $CH_3NH_3PbI_3$ perovskite solar cells

En-Dong Jia(贾恩东), Xi Lou(娄茜), Chun-Lan Zhou(周春兰), Wei-Chang Hao(郝维昌), Wen-Jing Wang(王文静)

Chin. Phys. B, 2017, 26 (**6**): 068803. DOI: 10.1088/1674-1056/26/6/068803

SPECIAL TOPIC — Emerging photovoltaic materials and devices

A silazane additive for $CsPbI_2Br$ perovskite solar cells

Ruiqi Cao(曹瑞琪)[1,2,†], Yaochang Yue(乐耀昌)[2,3,†], Hong Zhang(张弘)[2], Qian Cheng(程倩)[2], Boxin Wang(王博欣)[2], Shilin Li(李世麟)[2,3], Yuan Zhang(张渊)[3], Shuhong Li(李书宏)[1,‡], and Huiqiong Zhou(周惠琼)[2,§]

[1] *Beijing Technology & Business University, Department of Chemistry, Beijing* 100048, *China*

[2] *CAS Key Laboratory of Nanosystem and Hierarchical Fabrication, Nanoscience National Center for Nanoscience and Technology, Beijing* 100190, *China*

[3] *HEEGER Beijing Research & Development Center, Beihang University, Beijing* 100191, *China*

(Received 20 February 2022; revised manuscript received 24 May 2022; accepted manuscript online 27 June 2022)

Adding additives into peroskite precursor solution has been proven as a simple and efficient strategy to improve the quality of peroskite films. In this work, we demonstrate an effective additive strategy to improve the quality of all-inorganic perovskite films by adding a novel silazane additive heptamethyldisilazane (HDMS). The power conversion efficiency (PCE) of the optimized devices is enhanced from 14.55% to 15.31% with an open-circuit voltage over 1.26 V due to the higher quality perovskite films with lower trap density after the incorporation of HDMS. More interestingly, the HDMS devices exhibit superior humidity and thermal stability compared with the control ones. This work provides a simple and efficient strategy to enhance the device performance and stability of all-inorganic perovskite solar cells, which could facilitate its commercialization.

Keywords: silazane, all-inorganic perovskite, heptamethyldisilazane (HDMS), additive, solar cells

PACS: 01.50.Rt, 14.70.Bh **DOI:** 10.1088/1674-1056/ac7c01

1. Introduction

Since the first application of perovskite materials in solar cells in 2009, the power conversion efficiency (PCE) of organic–inorganic hybrid perovskite devices has exceeded 25% in only a few years.[1] While the thermal volatilization of methylamine ions (MA^+) in organic–inorganic hybrid perovskite makes it unstable, especially under high temperature and high humidity.[2–5] Theoreticlly, all-inorganic perovskite solar cells (PSCs) should exhibit better stability than the organic–inorganic hybrid halide ones by replacing the MA^+ with Cs^+.[6–9] However, the PCE of the all-inorganic perovskite solar cells is still much lower.

It is well-known that the device performance of PSCs strongly depends on the crystal quality of the perovskite photoactive layers. The incomplete grain boundaries between the perovskite crystals and a large number of defects at the interfaces will cause severe charge recombination, reducing charge mobilities and affecting the device stability.[13–15] Adding additives into peroskite precursor solutions has been proven as a simple and efficent strategy to improve the quality of peroskite films.[16–18] Heptamethyldisilazane (HDMS) is highly reactive, and can participate in various chemical reactions.[15,19] If chosen as an additive for perovskites, it could interact with the precursor and involve in the crytallization process of the perovskite, which might improve the crystallization and construct high quality perovskite films. In addition, HDMS also has certain hydrophobic properties,[19] which could improve the stability of the device in the external environment. Thus, it is expected to be used as an additive to improve the device efficiency and stability of perovskite solar cells.

In this work, we propose a simple method through incoporating a novel silazane additive HDMS into the perovskite precursor to improve the quality of all-inorganic perovskite films. Then we optimize the concentration of HDMS by checking the device performance of $CsPbI_2Br$ solar cells with various amount of additives. The best PCE of the opitimized devices with 1% HDMS is enhanced from 14.55% to 15.31% with a V_{OC} over 1.26 V. SCLC measurements and PL characterizations exhibit that the quality of the perovskite films is improved with lower trap density after the presence of HDMS. Moreover, the HDMS devices exhibit better humidity and thermal stability compared with the control ones. At the end, the influence of HDMS on the crystalization process of perovskite is explored.

2. Experimental procedures

2.1. Materials

Lead iodide (> 99.95%), lead bromide (> 99.95%), cesium iodide (> 99.95%) were purchased from Xi'an Polymer Light Technology Corp. Isopropanol (99.9%), ethanol (99.5%) and dimethyl sulfoxide (99.9%) were purchased from Alfa Aesar Chemical Co. SnO_2 nanoparticle solution (2.5 wt% SnO_2 in isopropanol) was purchased from Avantama. HDMS (97%) was purchased from Aladdin.

†These authors contributed equally.

‡Corresponding author. E-mail: lish@th.btbu.edu.cn

§Corresponding author. E-mail: zhouhq@nanoctr.cn

© 2022 Chinese Physical Society and IOP Publishing Ltd

2.2. Preparation of HDMS-$PbBr_2$

All compounds were weighed in the glove box, a certain amount of $PbBr_2$ and excess HDMS were mixed with each other, stirred for 1 h until $PbBr_2$ changed from white to yellow, then the excess HDMS was taken out, and the yellow powder was vacuum dried.

2.3. Film preparation and device fabrication

ITO glass substrates were cleaned sequentially with ethanol, detergent, deionized water, and acetone, followed by drying with N_2 flow and UV-ozone treatment for 15 min. The SnO_2 ($V_{SnO_2} : V_{H_2O} = 1 : 4$) was spin coating onto ITO at 4000 rpm for 30 s, then heating at 150 °C for 30 min. Precursor solution (467 mg of PbI_2, 361 mg of $PbBr_2$, and 312 mg of CsI were mixed in 1 mL of DMF and DMSO (1:9, v/v)) with different ratio of HDMS was spin coating at 2500 rpm for 25 s. Then annealing at 43 °C until the color became brown and annealing again at 180 °C for 10 min. The Spiro-OMeTAD in chlorobenzene solution (72.6 mg/ml) with 29 μL of 4-tert-butylpyridine, 17.5 μL of lithium bistrifluoromethylsulfonate (LiTFSI) was deposited onto the active layer by spin-coating at 4000 rpm for 30 s. Finally, the device was transferred to the evaporator for thermal evaporation of Au (60 nm–80 nm) at a pressure of 1×10^{-4} Pa.

2.4. Device testing and materials characterization

UV-vis spectra were measured by PerkinElmer Lambda 650/850/950 UV-vis spectrophoto-meter. X-ray diffraction (XRD, Rigaku D/MAX-TTRIII 3(CBO)) using Cu $K\alpha$ radiation was taken for the crystal structures. To acquire the morphology, we used the scanning electron microscope (SEM, Hitachi S4800). A fluorescence spectrophotometer (HORIBA Fluorolog-III) was used for PL spectra. The time-resolved photoluminescence (TRPL) of the films excited by 467 nm laser was obtained with TCSPC. Under AM 1.5 G illumination, current–voltage (J–V) characteristics of the photovoltaic devices were measured using an Enlitech SS-F5-3A. The J–V characteristics were measured with a Keithley 2400 source by Enlitech Ltd. For long-term operational stability test, we stored the solar cells in N_2 glove box and air.

3. Result and discussion

We fabricated $CsPbI_2Br$ films based on the perovskite precursor solutions containing various amounts of HDMS additive (molecular structure shown in Fig. 1(a)) via the one-step spin-coating procedure. Subsequently, we assembled solar cell devices with the structure of ITO/SnO_2/$CsPbI_2Br$(HDMS)/Spiro-OMeTAD/Au (see Fig. 1(b)). Figure 1(c) shows the current–voltage (J–V) curves of all-inorganic PSCs without additive and with different concentrations of HDMS. The detailed photovoltaic parameters are shown in Table 1. The optimized device with 1% HDMS shows the highest PCE of 15.31%, with a short circuit current (J_{SC}) of 15.39 mA/cm^2, an open-circuit voltage (V_{OC}) of 1.258 V, and a fill factor (FF) of 79.12%. It is worth noting that as the content of HDMS increases, the PCE of all-inorganic perovskite solar cells increases first and then decreases. Excess HDMS leads to complex crystallization paths, while promoting an adverse effect.[20,21] Therefore, subsequent studies were conducted between the 1% HDMS devices and the control ones. The external quantum efficiency (EQE) curve of the champion device is shown in Fig. 1(d), the tested J_{SC} of 15.25 mA/cm^2 is consistent with the previously mentioned in the J–V curve. The addition of HDMS seems to greatly improve the J_{SC} of the devices. Statistical diagram of the J_{SC} of 20 individual devices is described in Fig. 1(e). The optimized devices behave with good repeatability, and more than 80% of the devices have a J_{SC} of over 15 mA/cm^2, furthermore, the maximum J_{SC} of the device is over 15.5 mA/cm^2. Figure 1(f) investigates the stable power output (SPO) of the HDMS optimized device while tracking at the maximum power point, of whose efficiency for the optimized $CsPbI_2Br$ PSC is about 15.17% and the J_{SC} is 15.05 mA/cm^2.

The single carrier devices with the architecture of ITO/SnO_2/perovskite/C_{60}/BCP/Ag were fabricated as shown in Fig. S1 and the corresponding J–V curves are shown under dark condition to investigate the trap state density in the control and 1% HDMS films.

Compared with the control devices, obviously, the trap-filled limit voltages (V_{TFL}) for 1% HDMS tailored devices demonstrate a decreased trend. Due to the proportion of V_{TFL} to trap state density (N_{trap}),[22,23]

$$N_{trap} = \frac{2\varepsilon_0\varepsilon_r V_{tr}}{qL^2}, \tag{1}$$

where L is the thickness of the active layer, ε_0 is the vacuum permittivity, and ε_r is the dielectric constant of the perovskite. The determined N_{trap} can be assessed in Table 2, the device with HDMS has a smaller trap state density (4.712×10^{15} cm^{-3}), nearly half of the N_{trap} in the control one (7.603×10^{15} cm^{-3}). The reduced trap state density is due to the better crystallization in the all-norganic perovskite processed with HDMS.[24]

Table 1. Photovoltaic parameters of the $CsPbI_2Br$-based devices with different concentrations of HDMS.

Sample	V_{oc} (V)	J_{sc} (mA/cm^2)	FF (%)	PCE (%)
Control	1.22	14.83	80.32	14.55
0.1 % HDMS	1.21	14.89	77.72	14.05
0.2 % HDMS	1.23	15.11	80.25	14.99
0.5 % HDMS	1.26	15.39	77.41	15.04
1.0% HDMS	1.26	15.39	79.12	15.31
1.5 % HDMS	1.23	15.15	78.98	14.75
2.0 % HDMS	1.15	15.23	70.20	12.30

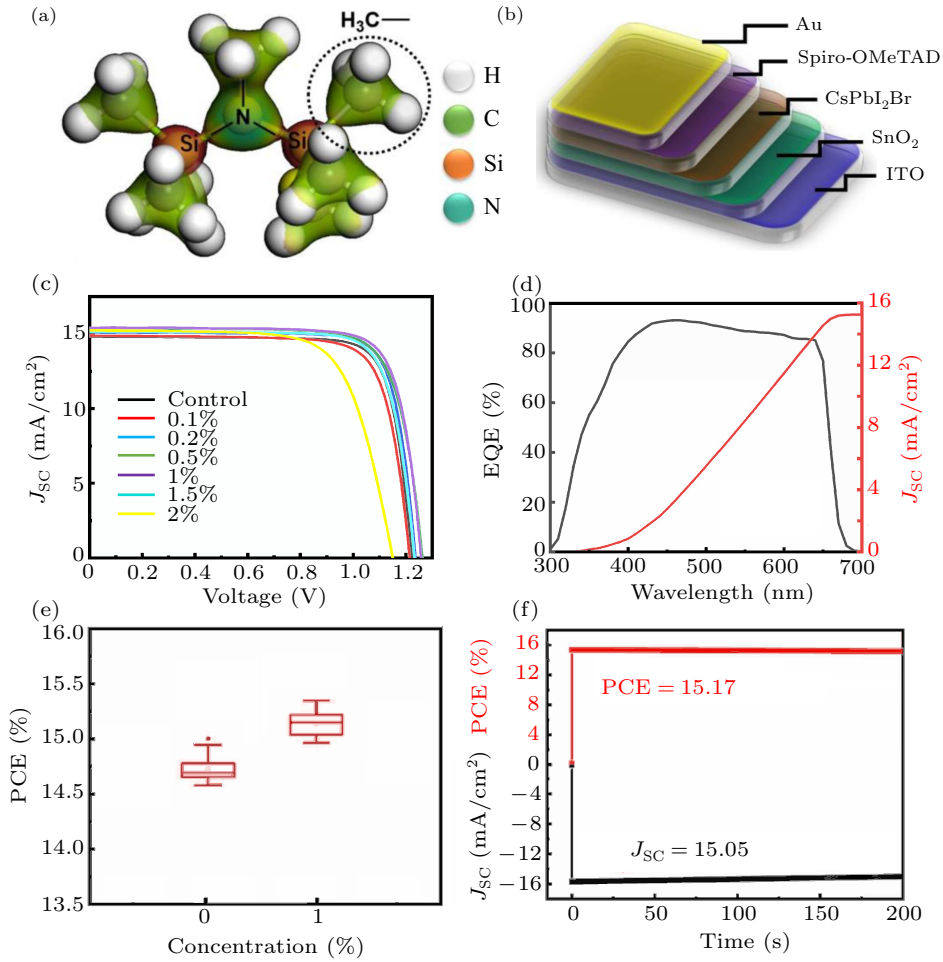


Fig. 1. (a) Structure of HDMS. (b) All-inorganic perovskite device structure. (c) *J*–*V* curves of the $CsPbI_2Br$-based devices with different concentrations of HDMS. (d) EQE curve and integrated J_{SC} of the champion device with 1% HDMS, (e) J_{SC} distributions for control devices (20 samples) and optimized $CsPbI_2Br$ PSCs (20 samples) with 1% HDMS, (f) the stable power output of the HDMS optimized device and long-term stability of the devices.

Table 2. TRPL parameters and defect state density of $CsPbI_2Br$ films with and without 1% HDMS-$PbBr_2$.

Sample	τ_1 (ns)	τ_2 (ns)	V_{tr} (V)	N_{trap} ($\times 10^{15}$) (cm^{-3})
Control	0.56	6.91	0.77	7.603
1% HDMS	0.40	8.40	0.33	4.712

As we all know, the performance of solar cells is related to the quality of the active layer. We also need to confirm the previous conjecture through film-related tests. Thus the perovskite films with or without HDMS were prepared. XRD was utilized to describe $CsPbI_2Br$ films after an annealing process. As shown in Fig. S2(a), both films show the same three main peaks at around 14.6°, 20.8° and 29.5°, which represent the (100), (110) and (200) planes of a typical $CsPbI_2Br$ cubic phase, respectively.[22,25–27] Meanwhile, the XRD peak positions which do not vary with the adding of HDMS demonstrate that HDMS is not inside the crystal.[28] To better indicate the morphology of the control and the 1%HDMS optimized perovskite films after an annealing process, SEM images (see Fig. S2(b)) were acquired, it shows that the optimized film possesses more smooth grain boundaries compared with the control.[20,29,30]

We then move to the optical properties of the additive on the quality of the pervskite film. To investigate trap states on the surface of the control and the optimized $CsPbI_2Br$ perovskite films, photoluminescence (PL) of both was studied (Fig. 3(a)). The stronger PL intensity compared with the control film means that there are less traps on the optimized surface.[31,32] Similarly, high quality films were revealed by single carrier devices (see Fig. 2), in which the unexpected charge recombination decreased. Also, a blueshift of the PL peak from 660 nm to 648 nm can be observed, which is resulted from that high quality perovskites film as confirmed by SCLC image can effectively reduce defect density.[33] Then the TRPL decays of the two $CsPbI_2Br$ perovskite thin films with and without HDMS were investigated. TRPL decay curves (Fig. 3(b)) were fitted by a bi-exponential decay function, and the key parameters of the two films are listed in Table 2. The average carrier lifetime (τ_{avg}) of two kinds of films are 0.58 ns and 3.82 ns, respectively. The much longer τ_{avg} of the optimized film also agrees with the conjecture of less trap states with the help of HDMS.[33,34]

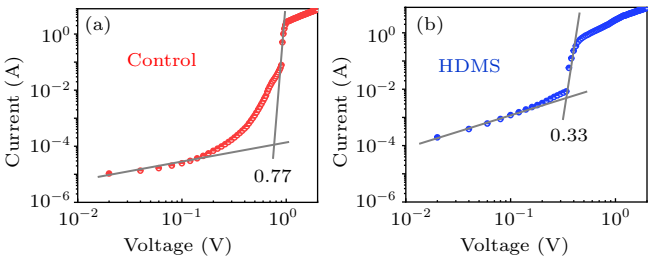


Fig. 2. The space-charge-limited current versus voltage of devices (a) without and (b) with 1% HDMS.

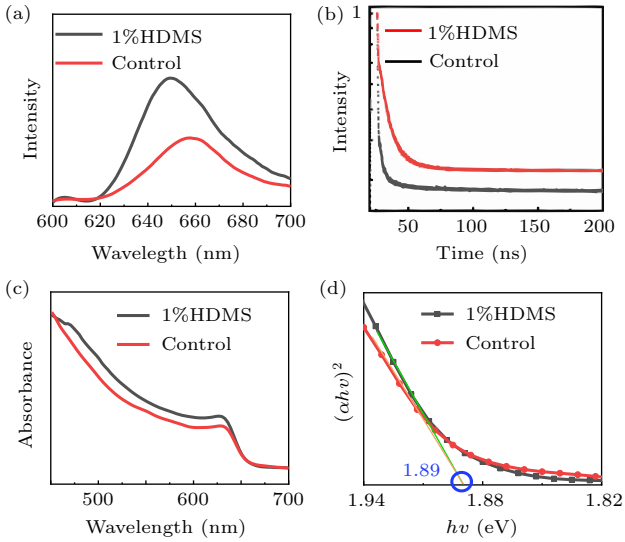


Fig. 3. (a) Steady-state PL spectra, (b) TRPL curves, (c) UV–vis absorption spectra, (d) Tauc plots of $CsPbI_2Br$ films with and without 1% HDMS.

Meanwhile, figure 3(c) shows the absorbance of the films with or without HDMS. The perovskite films with or without HDMS have almost the same absorption and the value is nearly 650 nm, which is consistent with the previous reports.[35] Using the Tauc method, the optical bandgap of these perovskite films is assessed in Fig. 3(d).[36] It is noted that a small amount of HDMS has no obvious effect on the bandgap of the $CsPbI_2Br$ perovskite film, and the values are both close to 1.89 eV, which is in line with the conclusions of other experiments. It should be noted that the HDMS film ($\approx$ 510 nm) is slightly thicker than the control film ($\approx$ 490 nm), which is the reason for the increased absorption strength.

Less traps promote the charge transport process,[36,37] and also enhance the stability of the perovskite devices.[38] Figure 4 demonstrates the long-term stabilities of the $CsPbI_2Br$ devices without encapsulation in the ambient atmosphere and thermal treatment, respectively. As shown in Fig. 4(a), the thermal stability of both devices at 85 °C in N_2 indicates that the optimized ones have an enhanced tolerance to high temperatures, especially for the decay time to 80% PCEs (control device of $\sim$ 70 h, HDMS one of $\sim$ 120 h). Figure 4(b) shows the humidity stability at 25 °C and RH 40%–50%. After 1000 h storing, the optimized devices with HDMS remained about 90% PCEs, while the devices without HDMS remained only 60%. These results suggest that HDMS is an effective additive to promote the film quality and prepare high PCE and stable PSCs. Figures 4(c) and 4(d) show the water droplet contact angles of the perovskite films with or without using additive. The contact angle for the optimized one is slightly larger than the control one. The superior device stability at high humidity might come from the enhanced hydrophobicity and the improved crystal quality of $CsPbI_2Br$ films with HDMS.

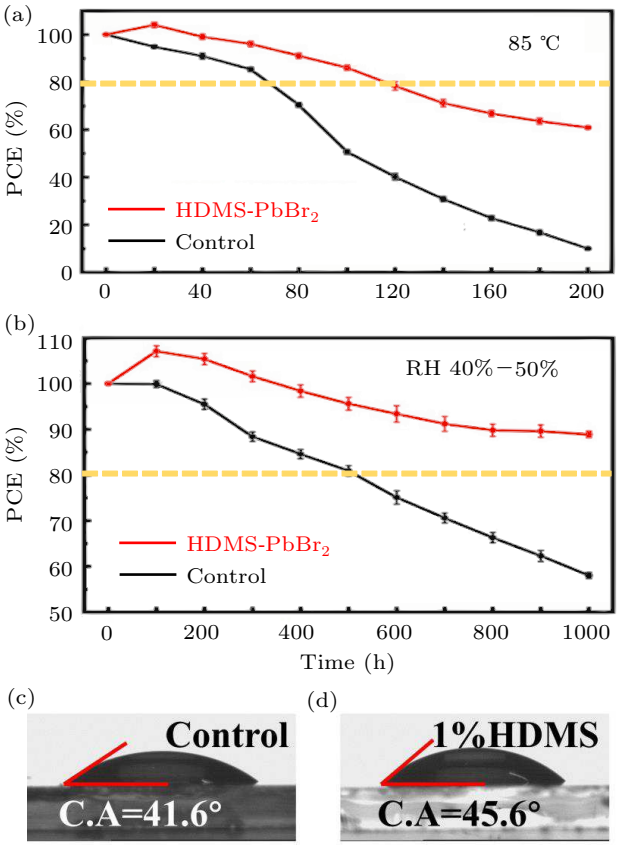


Fig. 4. Devices post stability of (a) RH 40%–50% in air and (b) 85 °C in N_2. The contact angle of (c) control film (d) film with 1%HDMS.

To figure out the influence of HDMS on the crystalization of perovskites, we explored a simplified experiment between HDMS and $PbBr_2$. Interestingly, the white $PbBr_2$ powder quickly turns into yellow after adding a certain amount of HDMS, and the color does not change after purification and drying, figure 5(a) shows the whole transformation. SEM characterization was carried out to check the mouphology change. As shown in Fig. 5(b), $PbBr_2$ powder exhibits bulk blocks, while HDMS-$PbBr_2$ shows much different morphology with small plate-shaped distribution. More importantly, there are many attachments which are considered to be HDMS in the figure of HDMS-$PbBr_2$. Then, we checked the XRD results (Figs. 5(c) and 5(d)). For the two samples, the main peaks between 20°–40° do not show any different, proving that there is no change in the inherent crystal structure ($PbBr_2$). While the new peak at below 20° in the HDMS sample might come from the coordination of HDMS with $PbBr_2$. Based on the

above experimental results, we suspect that the HDMS additive might firstly interact with $PbBr_2$ to form the HDMS–$PbBr_2$ complex, which could slow the reaction between $PbBr_2$ and CsI, resulting a higher-quality perovskite film. After the crystallization of $CsPbI_2Br$, the HDMS might serve as a surface modification component which adheres to the surface of the perovskite grains to improve the stability.

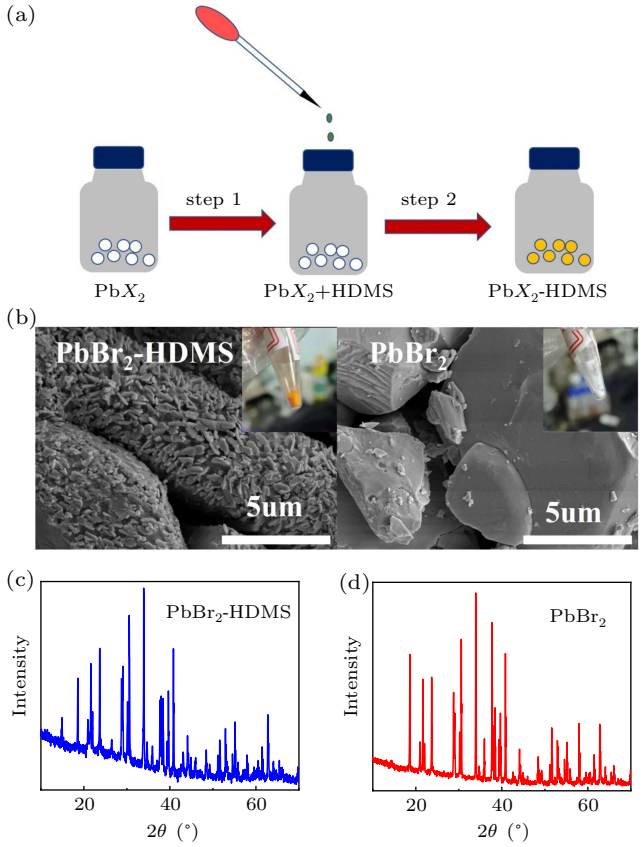


Fig. 5. (a) Preparation process of PbX_2-HDMS. Top-view SEM and physical diagram images of (b) $PbBr_2$-HDMS and $PbBr_2$. Powder XRD of (c) $PbBr_2$-HDMS and (d) $PbBr_2$.

4. Conclusion and perspectives

In summary, we demonstrate an effective additive strategy to improve the quality of all-inorganic perovskite films by adding a novel silazane additive HDMS into the perovskite precursor. The PCE of the optimized devices is enhanced from 14.55% to 15.31% with a V_{OC} over 1.26 V due to the higher quality perovskite films with lower trap density after the incoporation of HDMS. More interestingly, the HDMS devices exhibit better humidity and thermal stability compared with the control ones. This work provides a simple and efficient strategy to enhance the device performance and stability of all-inorganic perovskite solar cells, which could fercilitate its commercialization.

Acknowledgments

This work was financially supported by the National Key Research and Development Program of China (Grant No. 2017YFA0206600), the National Natural Science Foundation of China (Grant No. 21922505), and the Strategic Priority Research Program of Chinese Academy of Sciences (Grant No. XDB36000000).

References

[1] Yoo J J, Seo G, Chua M R, Park T G, Lu Y, Rotermund F, Kim Y K, Moon C S, Jeon N J, Correa-Baena J P, Bulovic V, Shin S S, Bawendi M G and Seo J 2021 *Nature* **590** 587
[2] Cheng Q, Xia H, Li X, Wang B, Li Y, Zhang X, Zhang H, Zhang Y and Zhou H 2021 *Solar rrl.* **6** 2100805
[3] Yue Y, Zhou J, Cheng Q, Zhang X, Wang B, Li Y, Li S, Cao R, Wang K, Wang H, Zhou H and Zhang Y 2021 *J. Phys. Chem. Lett.* **12** 11228
[4] Wu G, Yang T, Li X, Ahmad N, Zhang X, Yue S, Zhou J, Li Y, Wang H, Xinghua Shi, Liu S, Zhao K, Zhou H and Zhang Y 2020 *Matter* **4** 582
[5] Zhou Q, Wang B, Meng R, Zhou J, Xie S, Zhang X, Wang J, Yue S, Qin B, Zhou H and Zhang Y 2020 *Adv. Funct. Mater.* **30** 2000550
[6] Li X, Wu G, Wang M, Yu B, Zhou J, Wang B, Zhang X, Xia H, Yue S, Wang K, Zhang C, Zhang J, Zhou H and Zhang Y 2020 *Adv. Energy Mater.* **10** 2001832
[7] Li X, Wu G, Zhou J, Zhang J, Zhang X, Wang B, Xia H, Zhou H and Zhang Y 2020 *Small* **16** 1906997
[8] Xiang S, Li W, Wei Y, Liu J, Liu H, Zhu L and Chen H 2018 *Nanoscale* **10** 9996
[9] Wang K, Zhou J, Li X, Nafees A, Xia H, Wu G, Zhang X, Wang B, Zhang D, Zhou Y, Zhou H and Zhang Y 2020 *Phys. Chem. Chem. Phys.* **22** 17847
[10] Wu G, Liang R, Ge M, Sun G, Zhang Y and Xing G 2021 *Adv. Mater.* **34** 2105635
[11] Liu X, Zhang Z, Lin F and Cheng Y 2021 *InfoMat* **3** 1218
[12] Zhang D, Fan P, Shi J, Zheng Y, Zhong J and Yu J 2021 *Nano Res.* **14** 1319
[13] Zhou W, Chen Y and Zhou H 2021 *Acta Phys. Chim. Sin.* **37** 2009044
[14] Xia H, Li X, Zhou J, Wang B, Chu Y, Li Y, Wu G, Zhang D, Xue B, Zhang X, Hu Y, Zhou H and Zhang Y 2020 *ACS Appl. Energy Mater.* **3** 3186
[15] Wu G, Zhou J, Zhang J, Meng R, Wang B, Xue B, Leng X, Zhang D, Zhang X, Bi S, Zhou Q, Wei Z, Zhou H and Zhang Y 2019 *Nano Energy* **58** 706
[16] Kim B and Seok S I 2020 *Energy Environ. Sci.* **13** 805
[17] Chen W, Li X and Li Y 2020 *Energy Environ. Sci.* **13** 1971
[18] Jia X, Liu L and Fang Z 2019 *J. Mater. Chem. C* **7** 7207
[19] Kanda H, Shibayama N, Huckaba A J, Lee Y, Paek S, Klipfel N, Roldán-Carmona C, Queloz V I E, Grancini G, Zhang Y, Abuhelaiqa M, Cho K T, Li M, Mensi M D, Kinge S and Nazeeruddin M K 2020 *Energy Environ. Sci.* **13** 1222
[20] Wang B, Wu F, Bi S, Zhou J, Wang J, Leng X, Zhang D, Meng R, Xue B, Zong C, Zhu L, Zhang Y and Zhou H 2019 *J. Mater. Chem. A* **7** 23895
[21] You S, Wang H, Bi S, Zhou J, Qin L, Zhao Z, Xu Y, Zhang Y, Shi X, Tang Z and Zhou H 2018 *Adv. Mater.* **30** 1706924
[22] Han Y, Zhao H, Duan C, Yang S, Yang Z, Liu Z and Liu S 2020 *Adv. Funct. Mater.* **30** 1909972
[23] Wang Y, Qian D, Cui Y, Zhang H, Hou J, Vandewal K, Kirchartz T and Gao F 2018 *Adv. Energy Mater.* **8** 1801352
[24] Wang Q, Zhang W, Zhang Z, Liu S, Wu J, Guan Y, Mei A, Rong Y, Hu Y and Han H 2019 *Adv. Energy Mater.* **10** 1903092
[25] Wang X, Ran X, Liu X, Gu H, Zuo S, Hui W, Lu H, Sun B, Gao X, Zhang J, Xia Y, Chen Y and Huang W 2020 *Angew. Chem. Int. Ed.* **59** 13354
[26] Yin G, Zhao H, Jiang H, Yuan S, Niu T, Zhao K, Liu Z and Liu S F 2018 *Adv. Funct. Mater.* **28** 1803269
[27] Zhao H, Han Y, Xu Z, Duan C, Yang S, Yuan S, Yang Z, Liu Z and Liu S 2019 *Adv. Energy Mater.* **9** 1902279
[28] Wang H, Dong Z, Liu H, Li W, Zhu L and Chen H 2020 *Adv. Energy Mater.* **11** 2002940
[29] Tsai H, Nie W, Lin Y H, Blancon J C, Tretiak S, Even J, Gupta G, Ajayan P M and Mohite A D 2017 *Adv. Energy Mater.* **7** 1602159
[30] Qin Y, Zhong H, Intemann J J, Leng S, Cui M, Qin C, Xiong M, Liu F, Jen A K Y and Yao K 2020 *Adv. Energy Mater.* **10** 1904050

[31] Shi P, Ding Y, Ren Y, Shi X, Arain Z, Liu C, Liu X, Cai M, Cao G, Nazeeruddin M K and Dai S 2019 *Adv. Sci. (Weinh)* **6** 1901591
[32] Ye Q, Zhao Y, Mu S, Ma F, Gao F, Chu Z, Yin Z, Gao P, Zhang X and You J 2019 *Adv. Mater.* **31** 1905143
[33] Duan X, Li X, Tan L, Huang Z, Yang J, Liu G, Lin Z and Chen Y 2020 *Adv. Mater.* **32** 2000617
[34] Chen S, Zhang Y, Zhang X, Zhao J, Zhao Z, Su X, Hua Z, Zhang J, Cao J, Feng J, Wang X, Li X, Qi J, Li J and Gao P 2020 *Adv. Mater.* **32** 2001107
[35] Lau C F J, Zhang M, Deng X, Zheng J, Bing J, Ma Q, Kim J, Hu L, Green M A, Huang S and Ho-Baillie A 2017 *ACS Energy Lett.* **2** 2319
[36] Huang S H, Tian K Y, Huang H C, Li C F, Chu W C, Lee K M, Huang Y C and Su W F 2020 *ACS Appl. Mater. Interfaces* **12** 26041
[37] Bai D, Zhang J, Jin Z, Bian H, Wang K, Wang H, Liang L, Wang Q and Liu S F 2018 *ACS Energy Lett.* **3** 970
[38] Niezgoda J S, Foley B J, Chen A Z and Choi J J 2017 *ACS Energy Lett.* **2** 1043